Alloptical integrated Mach–Zehnder switching due to cascaded nonlinearities

Y. Baek, R. Schiek, G. I. Stegeman, G. Krijnen, I. Baumann et al.

Related Articles

Creation of diffraction-limited non-Airy multifocal arrays using a spatially shifted vortex beam
Appl. Phys. Lett. 102, 084103 (2013)

Low-voltage electro-absorption optical modulator based on slow-light Bragg reflector waveguide
Appl. Phys. Lett. 102, 031118 (2013)

Electro-optic properties of GaInAsSb/GaAs quantum well for high-speed integrated optoelectronic devices
Appl. Phys. Lett. 102, 013120 (2013)

Efficient terahertz electro-absorption modulation employing graphene plasmonic structures
Appl. Phys. Lett. 101, 261115 (2012)

High sensitivity differential magneto-optical imaging with a compact Faraday-modulator
Rev. Sci. Instrum. 83, 123906 (2012)

Additional information on Appl. Phys. Lett.

Journal Homepage: http://apl.aip.org/

Journal Information: http://apl.aip.org/about/about_the_journal

Top downloads: http://apl.aip.org/features/most_downloaded

Information for Authors: http://apl.aip.org/authors

All-optical integrated Mach–Zehnder switching due to cascaded nonlinearities

Y. Baek,[a)] R. Schiek, and G. I. Stegeman
Center for Research and Education in Optics and Lasers, University of Central Florida, 4000 Central Florida Boulevard, Orlando, Florida 32816

G. Krijnen
MESA Research Institute, University of Twente, Hengelose straat, 7500 AE, Enschede, the Netherlands

I. Baumann and W. Sohler
Angewandte Physik, Universität Paderborn, Warburger Strasse 100, D-33098 Paderborn, Germany

We demonstrate all-optical switching using the cascaded second order nonlinearity in a fully integrated, asymmetric Mach Zehnder interferometer implemented in lithium niobate channel waveguides. We obtained an 8:1 switching ratio. © *1996 American Institute of Physics.* [S0003-6951(96)02915-X]

In all optical switching, the required nonlinear phase shift is produced by the light itself. Typically this phase shift has been achieved via the intensity dependent refractive index, i.e., third order nonlinearities. But recently it was realized and verified experimentally that second order nonlinearities can yield large effective third order nonlinearities near the phase-matching conditions for second harmonic generation (SHG).[1–4] A phase shift in the cascaded nonlinearity is obtained through a spatially periodic energy exchange between a fundamental light beam and its second harmonic which propagate at different phase velocities.[5] During the process of the up-conversion to the second harmonic and the followed down-conversion to the fundamental, the fundamental light beam picks up the required phase shift for an all optical switching process. To date, we have demonstrated in LiNbO$_3$ channel waveguides that large phase shifts ($<1.5\pi$) are achievable with minimal ($<10\%$) net power loss to the second harmonic. Also reported has been all-optically controlled interference between two beams, one transmitted through a channel waveguide and the other through a reference arm in air, i.e., a hybrid Mach–Zehnder interferometer for all-optical switching has been demonstrated.[6] However, fully integrated versions of switching devices based on cascading are much more complex than their third order (Kerr) nonlinearity counterparts because there are four beams involved (two fundamentals and two second harmonics); phase matching is almost necessary, and the net conversion to second harmonic must be carefully controlled because it limits the efficiency of a cascaded device; i.e., is a loss to the fundamental throughput. Here we report the first implementation of a high contrast, cascading-based, all-optically switched, fully integrated asymmetric Mach–Zehnder interferometer.

A Mach–Zehnder interferometer requires a π relative phase shift between its two arms for switching, half of the phase shift needed for the nonlinear directional coupler also recently demonstrated via cascading.[6] In the fully integrated Mach–Zehnder interferometer, we can induce the required nonlinear phase difference between the two arms by design-ing the two channels to have different waveguide widths. As a result, each arm has a different effective mode index and cross-sectional area. Therefore, when temperature is used to achieve phase matching for SHG, each arm requires a different phase-matching (resonance) temperature, which in turn induces the different nonlinear phase shift needed in each channel for switching at a fixed temperature.

Based on the above philosophy, we designed a 50 mm long titanium indiffused asymmetrical lithium niobate channel waveguide with propagation direction along the X axis of a Y-cut crystal. The waveguides were produced by indiffusion of 43 nm thick titanium stripes at a temperature of 1060 °C for 9 h. The end surfaces were polished for end fire coupling. A 5° tilt of the outcoupling surface was made to prevent longitudinal cavity mode resonances. A Nd:YAG Q-switched and mode-locked laser operating at 1.32 μm with a repetition rate of 500 Hz was used. The full width at the half maximum intensity of the pulses was 90 ps. An electro-optic pulse slicer was used to extract a single pulse from each Q-switched envelope to eliminate thermal effects. Two half-wave plate and polarizer pairs were used to control the input power. Input and output signals were measured separately using fast Ge detectors and boxcar integrators.

The integrated Mach–Zehnder interferometer consists of two symmetric Y junction (Fig. 1). At the first Y junction, the input beam is equally split into each of the two arms. In one arm, the width of the channel waveguide is tapered down from 15 to 11 μm. The separation between two arms is 80 μm, which is wide enough to prevent linear coupling. At the second Y junction, the light from two channels is recombined, causing interference effects. Because of the difference in the widths of the two interferometer arms, different amounts of the nonlinear phase shift occur in each arm at a fixed temperature, as discussed previously. Type I birefringent phase matching between the TM$_{00}$ modes of the fundamental and TE$_{00}$ modes of the second harmonic at a temperature of around 346 °C was designed into the structure. A crystal oven was used to heat the sample to near the phase-matching temperature. With small variations in the radius of the Y-junction bends, resulting in small changes in the length of the branches at fixed sample length, we were able to ob-
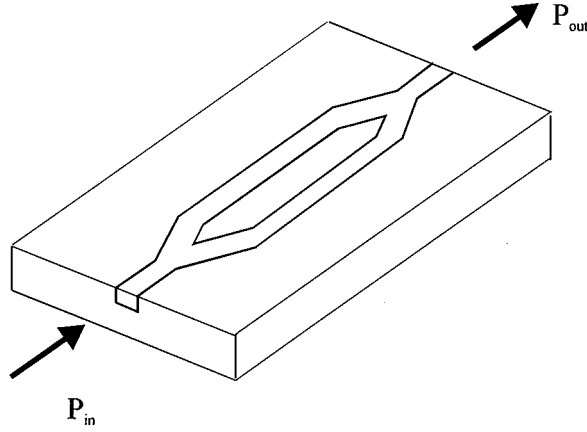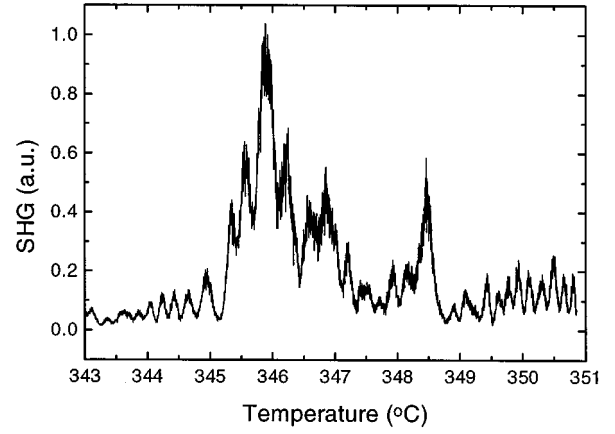
FIG. 1. Configuration of the integrated Mach–Zehnder interferometer.

FIG. 2. Measured temperature dependence of SHG for a peak input power of 150 W. (The first peak around 346 °C corresponds to the 15 μm arm and the second one around 348.5 °C corresponds to the 11 μm arm.)

tain different initial linear phase differences between the channels of approximately zero and π.

First, we measured the efficiency and tuning curves for SHG from a 15 μm wide single reference waveguide on the same sample in order to evaluate the effective temperature (and hence wave vector mismatch) profile along the waveguide. The temperature profile in the oven and a slight waveguide inhomogeneity provide the nonuniform wave vector mismatch distribution along the propagation length.[4] Due to this nonuniform wave vector mismatch, we can obtain large nonlinear phase shift along with small fundamental depletion, ideal for an efficient all-optical switching device. The effective temperature profile along the waveguide can be approximated by

$$T = T_{\text{SET}} + \Delta T_P - 0.35 \ K \left\{ 1 - \exp\left[-\left(\frac{z/\text{mm} - 25}{2.733} \right)^2 \right] \right\},$$

with

$$\Delta T_P / K = \begin{cases} \left(\dfrac{12.5 - z/\text{mm}}{5} \right)^2, & \text{for } z \leq 12.5 \ \text{mm}, \\ 0, & \text{for } 12.5 \ \text{mm} < z \leq 37.5 \ \text{mm}, \\ \left(\dfrac{z/\text{mm} - 37.5}{5} \right)^2, & \text{for } 37.5 \ \text{mm} < z. \end{cases}$$

T_{SET} is the set-point temperature for the crystal oven controller in °C.

To test our results against theory, we modeled the wave propagation in the Mach–Zehnder interferometer using coupled mode theory:

$$\frac{dA_F}{dz} + i\beta_F(z)A_F = -\frac{i\omega_F \varepsilon_0}{4p_0} K(2\chi^{(2)} A_{\text{SH}} A_F^*) - \frac{\alpha}{2} A_F,$$

$$\frac{dA_{\text{SH}}}{dz} + i\beta_{\text{SH}}(z)A_{\text{SH}} = -\frac{i\omega_{\text{SH}} \varepsilon_0}{4p_0} K(\chi^{(2)} A_F A_F)$$
$$- \frac{\alpha_{\text{SH}}}{2} A_{\text{SH}}. \tag{1}$$

Equation (1) describes the development of the fundamental $|A_F|^2 p_0$ and second harmonic powers $|A_{\text{SH}}|^2 p_0$ in units of $p_0 = 1$ W along the waveguide axis z for cw excitation. The α's are the linear loss coefficients, $\alpha_F = 0.04$ cm^{-1} and

$\alpha_{\text{SH}} = 0.08$ cm^{-1}, and $\chi^{(2)} = \chi^{(2)}_{ZYY} = -5.6$ pm/V is the applicable second order susceptibility tensor element in LiNbO$_3$. $K = \iint dx \, dy \, e_F e_F e_{\text{SH}}^*$ is the overlap integral. With a finite-difference program, the modal fields and the temperature- and wavelength-dependent propagation constants, β's, are calculated. Modification of the propagation constants and
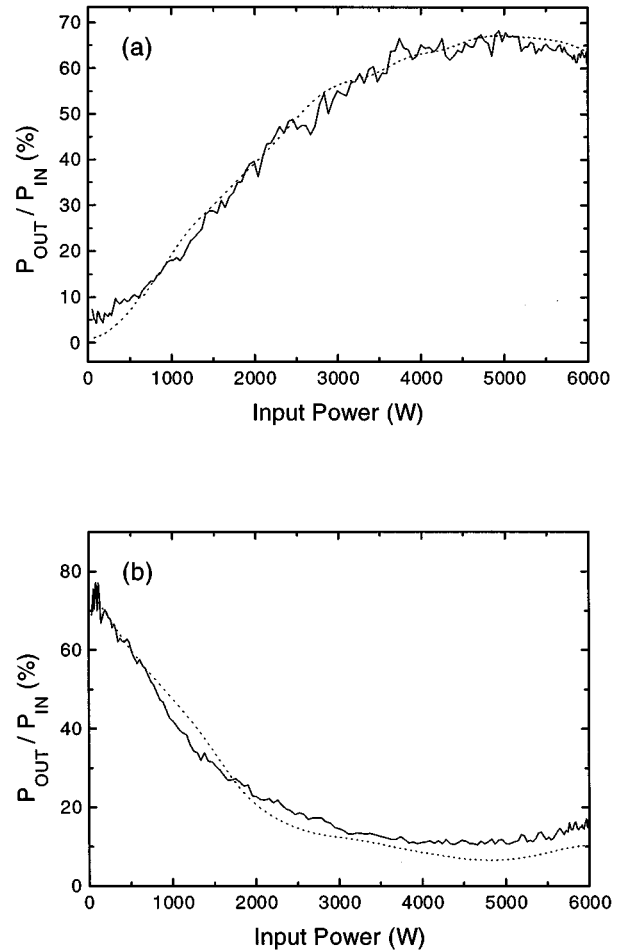

FIG. 3. Measured transmittance of a LiNbO$_3$ integrated Mach–Zehnder interferometer at $T = 344$ °C as a function of the peak input power: (a) initial relative phase between the interferometer arms of $\cong \pi$; (b) initial phase of $\cong 0$ (solid curves, experiment; dotted curves, theory).

overlap integral due to the designed changes in the waveguide geometry were taken into account. At the Y junction, we assume the power is divided equally into each arm, which is also verified experimentally in reference Y-junction waveguide. The losses due to the Y junctions and taperings were also calculated using beam propagation methods and included in the simulation. The pulsed light experiments were simulated on the basis of Eq. (1) with additional averaging over the temporal pulse profile, assuming the pulses are long enough so that temporal dispersion can be neglected. For our experiments, this approximation is valid.

We measured the SHG versus temperature at low input powers to find the resonance temperatures of each arm. The measured SHG tuning curves show two resonance temperatures separated by 2.5 K (Fig. 2). We chose the temperature of the switching experiments to be around 344 °C, which is in the low depletion region below both phase-matching temperatures. Figure 3 shows the fundamental output of the Mach–Zehnder interferometer, normalized to the input power. Due to the differences in the effective length of the arms, the switching curves start either in the ''on'' or ''off'' conditions. As we increased the input power, due to the cascaded second order nonlinearity, the difference in amounts of the induced phase shift of each arm increases. Therefore, the output is changed from ''on'' to ''off'' or vice versa. Pulse breakup is responsible for the incomplete switching. However, because of the nonlinear dependency of the phase shift on the input power in the cascaded second order nonlinearities, we obtained a better switching ratio than usually achieved with third order nonlinear materials.[7,8] In our waveguide geometry, the actual length of the arms that contribute to the generated phase differences is only 18 mm. Also, because the separation of the two resonances is only 2.5 K, the

nonlinear phase shift from the 11 μm wide arm is not zero and is still significant at the switching temperature. Consequently, the switching power was much higher than for the previous hybrid switching case.[9] In general, the results were in good agreement with the simulations.

In conclusion, we have reported all optical switching in a fully integrated Mach–Zehnder interferometer due to the cascaded second order nonlinearities with a switching ratio of 8:1. To the best of our knowledge, along with the previously mentioned lithium niobate directional coupler, these represent the first integrated all-optical switching devices using cascaded second order nonlinearities.[6] By using a higher $\chi^{(2)}$ material and/or quasiphase-matching techniques independently for each channel, we can reduce the switching power by orders of magnitude.

[1] R. DeSalvo, D. J. Hagan, M. Sheik-Bahae, G. I. Stegeman, E. W. Van Stryland, and H. Vanherzeele, Opt. Lett. **17**, 28 (1992).
[2] G. I. Stegeman, M. Sheik-Bahae, E. W. Van Stryland, and G. Assanto, Opt. Lett. **18**, 13 (1993).
[3] M. L. Sundheimer, C. Bosshard, E. W. Van Stryland, G. I. Stegeman, and J. D. Bierlein, Opt. Lett. **18**, 1397 (1993).
[4] R. Schiek, M. L. Sundheimer, D. Y. Kim, Y. Baek, G. I. Stegeman, H. Seibert, and W. Sohler, Opt. Lett. **19**, 1949 (1994).
[5] A. Armstrong, N. Bloembergen, J. Ducuing, and P. S. Pershan, Phys. Rev. **127**, 1918 (1962).
[6] R. Schiek, Y. Baek, G. I. Stegeman, I. Baumann, and W. Sohler (unpublished).
[7] B. K. Nayer, N. Finlayson, N. J. Doran, S. T. Davey, D. L. Williams, and J. W. Arkwright, Opt. Lett. **16**, 408 (1991).
[8] K. Al-Hemyari, J. S. Aitchison, C. N. Ironside, G. T. Kennedy, R. S. Grant, and W. Sibbett, Electron. Lett. **28**, 1090 (1992).
[9] Y. Baek, R. Schiek, and G. I. Stegeman, Opt. Lett. **20**, 2168 (1995).